

Chapter 5 CRYSTALLIZATION KINETICS OF METALLIC GLASSES AND ZBLAN GLASS

5.1 Introduction

The metallic glasses, which are kinetically metastable, can be transformed into crystalline state by both isothermal and non-isothermal methods. Thermal analysis methods are widely used to study the crystallization kinetics of amorphous materials. The study of this transformation and hence the thermal stability of metallic glasses are important from the application view point. In the present chapter, the crystallization of two materials, one is ZBLAN glass and the other one is 2714A metallic glass is studied under non-isothermal conditions using DSC. The Avrami exponent (n), Frequency factor (A) and Activation Energy (E) of crystallization are evaluated using different isokinetic as well as isoconversional methods.

The study of crystallization process of metallic glass forming alloys is important in understanding amorphization in metallic systems. The properties of fully or partly crystalline materials usually differ from those of the corresponding amorphous materials. Thus, the kinetics of crystallization must be known to attain products with required fraction crystallized or to avoid the degradation of materials when they are cooling from high processing temperatures. Crystallization kinetics is extensively studied by thermal analysis methods.

A full kinetic analysis of a solid state reaction has at least two major stages:

Experimental collection of data:

Different thermal analysis methods like Differential Scanning Calorimetry (DSC) or differential thermal analyzer (DTA) are performed to get the data which is suitable for adequate kinetic analysis. The DSC/DTA experiments can be carried out in isothermal as well as isochronal (non-isothermal) conditions. The choice of the mode of experiment to study the kinetics of the phase transformation has always been a matter of debate due to their relative advantages and inherent limitations. Though the isothermal techniques are definitive in most case, the non-isothermal techniques possess several advantages over it. Some of the notable advantages of the non-isothermal techniques are: (i) the rapidity with which the experiment can be performed (ii) extended temperature range of measurements beyond those accessible

to isothermal experiments. Further, many phase transformations occur too rapidly to be measured under isothermal conditions because of transients inherently associated with the experimental apparatus [1]. Non-isothermal transformation kinetics becomes important in such instances.

i) *Computation of kinetic characteristics for the data from 1st stage:*

The data obtained using different thermo analytical techniques is usually in one of the following forms:

- Sets of α , t (or $d\alpha/dt$, t) data at several different constant temperatures.
- Sets of α , T (or $d\alpha/dt$, T or $d\alpha/dT$, T) data at several different constant heating rates β .
- Sets of T , t data obtained at several different constant reaction rates $d\alpha/dt$.

Here α is the volume fraction of the sample reacted, for example the volume transformed in crystalline phase during the crystallization event, and can be obtained from DSC curve as a function of temperature (T).

The analysis of the data is usually sought in terms of a kinetic triplet, E - the activation energy, A - the pre-exponential factor and $f(\alpha)$ - the reaction model or the conversion function. Each of these parameters represents an important physical concept. For example the transition state theory links E to the energy barrier and A to the vibrational frequency of the activated complex. Numerous solid state reaction models link $f(\alpha)$ to the reaction mechanism. Therefore, by the evaluation of the kinetic triplet one can theoretically interpret the experimental data. Practically, this kinetic triplet provides a mathematical description of the process. If the kinetic triplet is determined correctly, it can be used to reproduce the original kinetics data as well as to predict the process kinetics outside the experimental temperature region.

To determine the kinetic parameters of the crystallization processes the choice of a sound method for the analysis of the experimental data is important. A multitude of methods for the kinetic analysis are available in the literature. These methods are

generally based on either the isokinetic hypothesis or the isoconversional principle and they can be accordingly categorized as:

(1) Isokinetic methods

(2) Isoconversional methods

In the isokinetic methods the transformation mechanism is assumed to be the same throughout the temperature/time range of interest and, the kinetic parameters are assumed to be constant with respect to time and temperature whereas the isoconversional methods assume that the reaction rate at a constant extent of conversion is only a function of temperature. The kinetic parameters, in isoconversional analysis, are considered to be dependent on the degree of transformation at different temperature and time.

Experimental work

The Differential Scanning Calorimetry (DSC) is used for collecting the data required for kinetic analysis. The heat flux type of DSC (DSC-50, Shimadzu, Japan) is utilized. The DSC scans were recorded by a thermal analyzer (TA-50 WSI, Shimadzu, Japan) interfaced to a computer. The detection sensitivity of the instrument is $\sim 10 \mu\text{W}$. The heat transformations and other essential physical quantities were obtained from the thermograms with the help of software, provided with the equipment. In DSC-50, the exothermic events are displayed by the upside shift of the baseline.

Specimens of amorphous ZBLAN glass were cut into small pieces and crimped in aluminum pans and loaded in the DSC cell with the reference material α – alumina. The DSC runs were carried out on these samples at four linear heating rates (5, 10, 15 and 20 Kmin^{-1}) from room temperature to 673K in air.

Methods of analysis of the experimental data

The rate of solid state reaction is generally described by [2]

$$\frac{d\alpha}{dt} = k(T)f(\alpha) = A \exp\left(-\frac{E}{RT}\right) f(\alpha) \quad (5.1)$$

where $k(T)$ is the reaction rate constant, $f(\alpha)$ is the reaction model, α is the conversion fraction, A is the preexponential factor, E the activation energy and R the gas constant.

Isoconversional Methods

Isoconversional methods calculate E values at progressive degrees of conversion without modelistic assumptions. These methods can be broadly classified into two categories: (1) Linear methods and, (2) Non-linear methods. The linear integral methods can further be classified into integral and differential methods. The isoconversional methods are based on the basic kinetic equation given by Eq.(5.1). The integral form of Eq.(5.1) is expressed as:

$$g(\alpha) = \frac{A}{\beta} \int_0^T \exp\left(-\frac{E}{RT}\right) dT \equiv \frac{AE}{\beta R} p(x) \quad (5.2)$$

where $x = E/RT$ and $p(x)$ is the temperature integral which cannot be calculated exactly. Hence different researchers used different approximations to calculate the temperature integral.

5.3.1.1 Linear Integral Isoconversional Methods

[1] *Ozawa-Flynn-Wall (OFW) method* [3, 4]:

In this method, the temperature integral in Eq.(5.2) is approximated to be equal to $(-E/RT)$ which further simplifies Eq.(5.2) in the following form.

$$\ln \beta = \ln \left(\frac{AE}{Rg(\alpha)} \right) - 1.052 \frac{E}{RT} - 5.331 \quad (5.3)$$

The factor 1.052 is a correction factor. The value of activation energy can be determined from the plot of $\ln\beta$ as a function of $(1/T)$.

At $T=T_p$ (peak temperature), Eq.(5.3) reduces to Ozawa equation.

[2] *Kissinger-Akahira-Sunose (KAS) Method* [5]:

According to the Murray and White approximation [6], the temperature integral can be approximated to be $\exp(-y^2)/y^2$, y being E/RT . Using this approximation in Eq.(5.2) results in the KAS equation

$$\ln\left(\frac{\beta}{T^2}\right) = \ln\left(\frac{AR}{Eg(\alpha)}\right) - \frac{E}{RT} \quad (5.4)$$

The slope of the plot of $\ln(\beta/T^2)$ Vs. $1/T$ leads to the value of the activation energy.

The general equation for the special cases of KAS method when $T= T_p$ is written as

$$\ln\left(\frac{\beta}{T_p^s}\right) = -Z \frac{E}{RT_p} + \text{const.} \quad (5.5)$$

When (1) $s = 2$ and $Z = 1$ Eq. (5.5) reduces to *Kissinger equation*

(2) $s = 1$ and $Z = 1$ Eq. (5.5) reduces to *Bosewell equation*

(3) $s = 0$ and $Z = 1.052$ Eq. (5.5) reduces to *Ozawa equation*

Another special case of KAS is suggested by *Augis and Bennett* [7] as

$$\ln\left(\frac{\beta}{(T_p - T_o)}\right) = -\frac{E}{RT_p} + \ln A \quad (5.6)$$

where T_p and T_o are the peak and onset temperatures respectively. To estimate the value of Avrami exponent, n also, Augis and Bennett have derived an equation as

$$n = \frac{2.5 T_p^2}{\Delta T \frac{E}{R}} \quad (5.7)$$

where ΔT is the full width at half maximum of the DSC curves.

[3] *Li-Tang method* [8]:

This method also does not need to make any assumption about the kinetic model and involves no approximation to the temperature integral. It is based on the following equation.

$$\int_0^\alpha \ln \left(\frac{d\alpha}{dt} \right) d\alpha = G(\alpha) - \frac{E}{R} \int_0^\alpha \left(\frac{1}{T} \right) d\alpha \quad (5.8)$$

where
$$G(\alpha) \equiv \alpha \ln A + \int_0^\alpha \ln f(\alpha) d\alpha$$

5.3.1.2 *Linear Differential Isoconversional Methods*

[1] *Friedman method* [9]:

The method suggested by Friedman, utilizes the differential of the transformed fraction and hence it is called differential isoconversional method. According to this method, taking logarithm on both sides of Eq.(5.1), we obtain

$$\ln \left(\frac{d\alpha}{dt} \right) = \ln \left(\beta \frac{d\alpha}{dT} \right) = \ln (A f(\alpha)) - \frac{E}{RT} \quad (5.9)$$

The activation energy can be easily determined from the slope of the plot of $\ln \beta (d\alpha/dt)$ Vs. $(1/T)$. This method, does not take any mathematical approximation for the temperature integral.

[2] *Gao and Wang Method* [10]

The special case of Friedman method is suggested by Gao and Wang, at $T = T_p$, and is expressed as

$$\ln \left[\beta \left(\frac{d\alpha}{dT} \right)_p \right] = -\frac{E}{RT_p} + \text{const} \quad (5.10)$$

The frequency factor and the Avrami exponent, from this method, can be determined using the following expressions

$$K_p = \frac{\beta E}{RT_p^2} \quad (5.11)$$

where
$$K_p = A \exp \left(\frac{-E}{RT_p} \right)$$

$$n = \frac{\left(\frac{d\alpha}{dt} \right)_p}{0.37 K_p} \quad (5.12)$$

5.3.1.3 Non-linear isoconversional method:

For non-isothermal experiments, a non-linear method developed by Vyazovkin [11], avoids inaccuracies associated with analytical approximations of the temperature integral. For a set of m experiments carried out at different heating rates, the activation energy can be determined at any particular value of α by finding the value of $E(\alpha)$ for which the function

$$\sum_{i \neq j}^m \sum_{j=1}^m \frac{[I(E_\alpha, T_{\alpha i}) \beta_j]}{[I(E_\alpha, T_{\alpha j}) \beta_i]} = \text{minimum} \quad (5.13)$$

The minimization procedure can be repeated for each value of α and hence the dependence of E on α can be studied.

5.3.2 Isokinetic Methods

The isokinetic methods of kinetic analysis depend on the reaction model and hence are also called as model fitting methods. These methods rely on the isokinetic hypotheses to separate the kinetics of the transformation from its dependence on temperature. Different isokinetic methods are described below;

Matusita and Sakka method

Matusita and Sakka [12] suggested the following equation specifically for the non-isothermal data

$$\ln[-\ln(1-\alpha)] = -n \ln \beta - \frac{mE_c}{RT} + Const \quad (5.14)$$

where m is an integer depends on the dimensionality of the crystal and the Avrami exponent n depends on the nucleation process. For a constant temperature, the plot of $\ln[-\ln(1-\alpha)]$ Vs. $\ln \beta$ gives a straight line and the slope gives the value of n . The value of activation energy E can be obtained from the plot of $\ln[-\ln(1-\alpha)]$ Vs. $1/T$ at constant heating rate.

5.3.2.1 Modified Kissinger method

The modified Kissinger equation [13] given below can be utilized to derive the activation energy.

$$\ln \left(\frac{\beta^n}{T_p^2} \right) = -\frac{mE}{RT_p} + Const \quad (5.15)$$

In order to derive E from this equation, one must know the value of n . The n value can be obtained from the slope of the plot of $\ln[-\ln(1-\alpha)]$ Vs. $\ln\beta$ at constant temperature.

The plots of $\ln\left(\frac{\beta^n}{T_p^2}\right)$ Vs. $1/T_p$, for different n values obtained, give the values of activation energy E .

Coats & Redfern method

One of the most popular model-fitting methods is the Coats and Redfern method [14]. This method is based on the equation

$$\ln \frac{g_j(\alpha)}{T^2} = \ln \left[\frac{A_j R}{\beta E_j} \left(1 - \frac{2RT}{E_j} \right) \right] - \frac{E_j}{RT} \cong \ln \frac{A_j R}{\beta E_j} - \frac{E_j}{RT} \quad (5.16)$$

where E_j and A_j are the Arrhenius kinetic parameters corresponding to a particular reaction model $g_j(\alpha)$. The graph of $\ln\left(\frac{g_j(\alpha)}{T^2}\right)$ Vs. $1/T$ gives a straight line whose slope and intercept allow us to calculate E and A for a particular reaction model.

5.3.2.4 The invariant kinetic parameter (IKP) method

It has been observed that the same experimental curve $\alpha = \alpha(T)$ can be described by different function of conversion ($f(\alpha)$). Further, the values of the activation energy obtained for various $f(\alpha)$ for single non-isothermal curve are correlated through the compensation effect [15]. These observations form the basis of the IKP method. In order to apply this method, $\alpha = \alpha(T)$ curves are obtained at different heating rates for each heating rate the pairs (A_{vj}, E_{vj}) , where j corresponds to a particular degree of conversion, are determined using the following equation:

$$\ln \frac{g(\alpha)}{T^2} = \ln \frac{AR}{\beta E} - \frac{E}{RT} \quad (5.17)$$

For constant β , a plot of $\ln\left(\frac{g(\alpha)}{T^2}\right)$ Vs. $1/T$ is a straight line whose slope allows the evaluation of activation energy E_v and intercept, pre-exponential factor, A for different reaction models $g(\alpha)$. The same procedure is repeated to obtain the pairs (E_v, A_v) for different heating rates. Now, the calculation of invariant activation parameters is done using the compensation relation

$$\ln A_v = \alpha^* + \beta^* E_v \quad (5.18)$$

The Eq.(5.18) represents a linear relationship between $\ln A$ and E ; any increase in the magnitude of one parameter is offset, or compensated, by appropriate increase of the other. Plotting $\ln A_v$ Vs. E_v for different heating rates, the compensation effect parameters α^* and β^* are obtained. These parameters follow an equation [16]

$$\alpha^* = \ln A - \beta^* E \quad (5.19)$$

The plot of α^* and β^* gives the true values of E and A .

Results and Discussions

5.4.1 ZBLAN glass

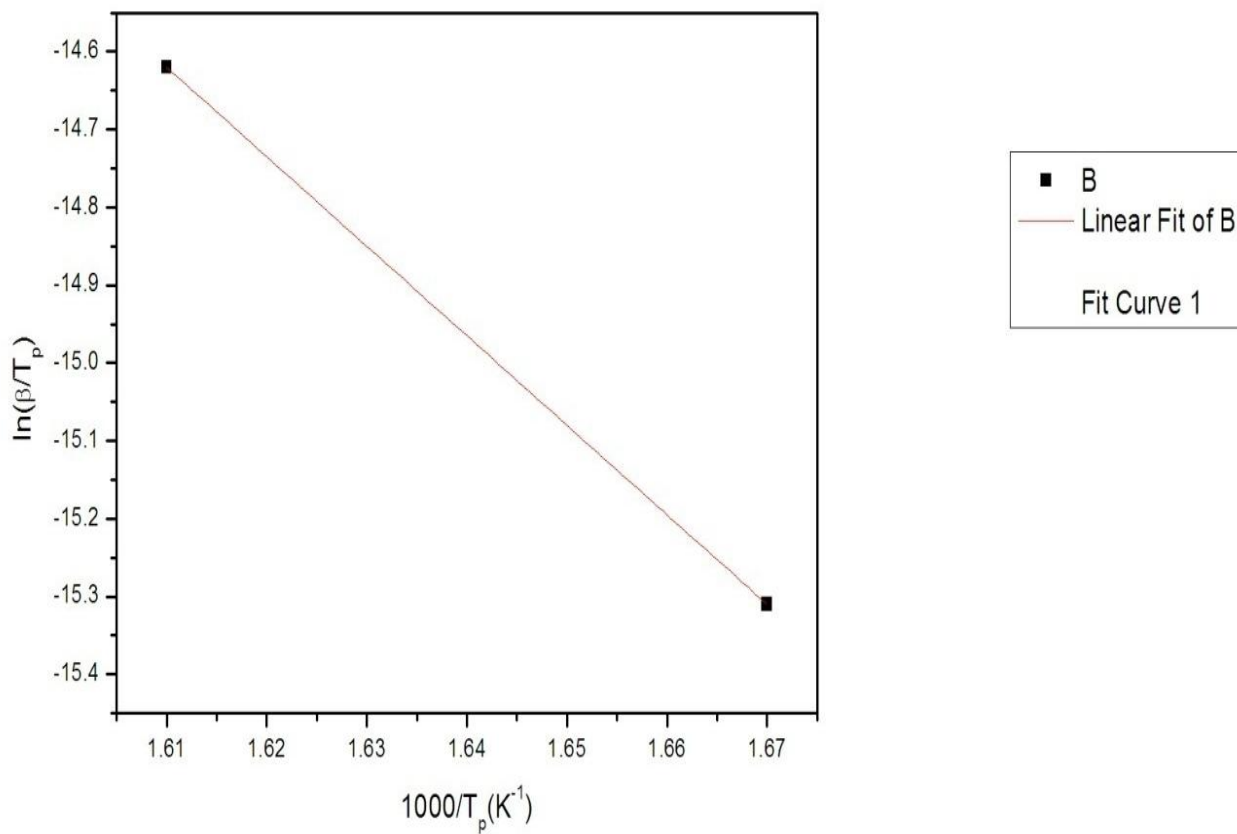


fig. 5.1: Kissinger plot for ZBLAN glass

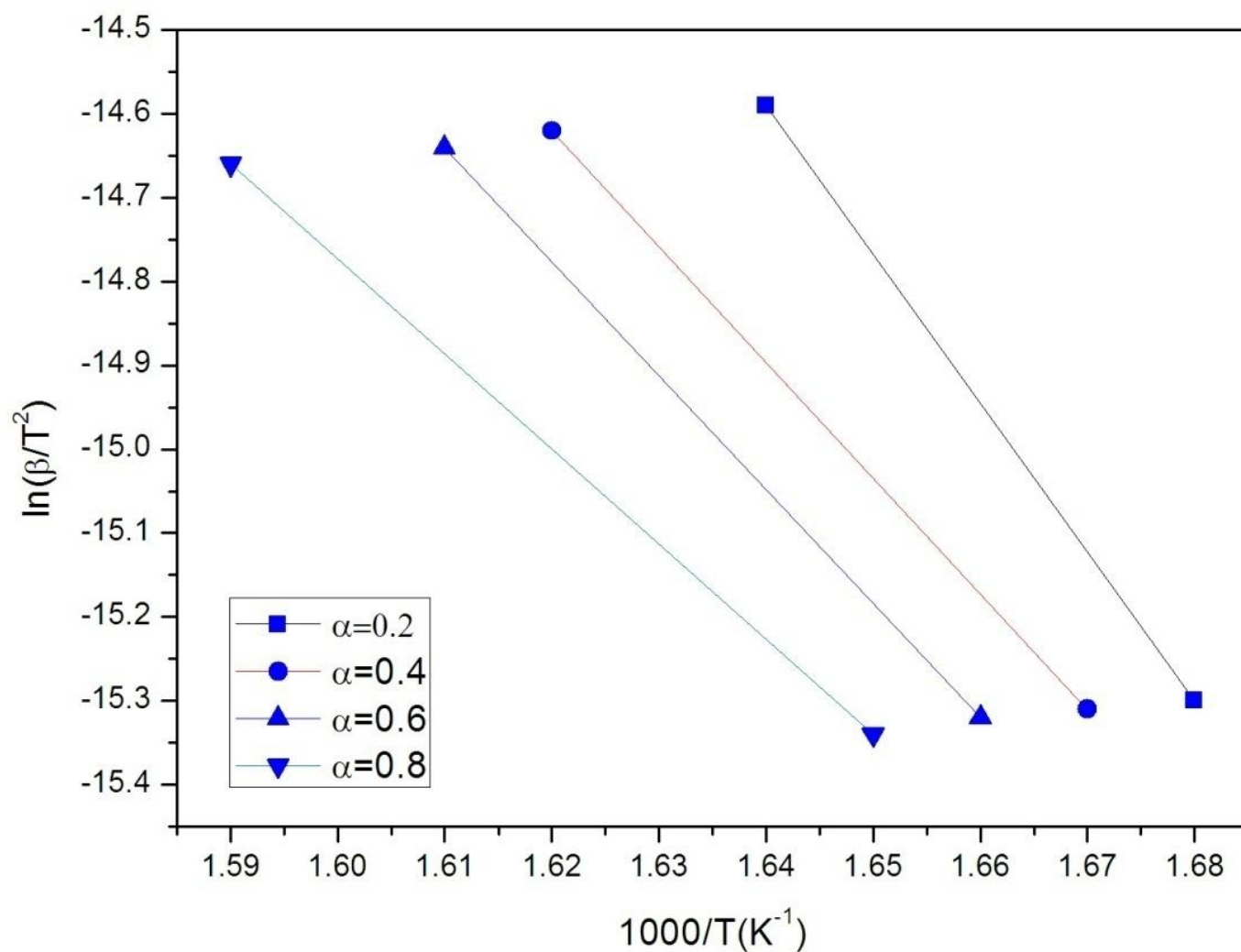


Fig. 5.2: KAS plots for ZBLAN glass

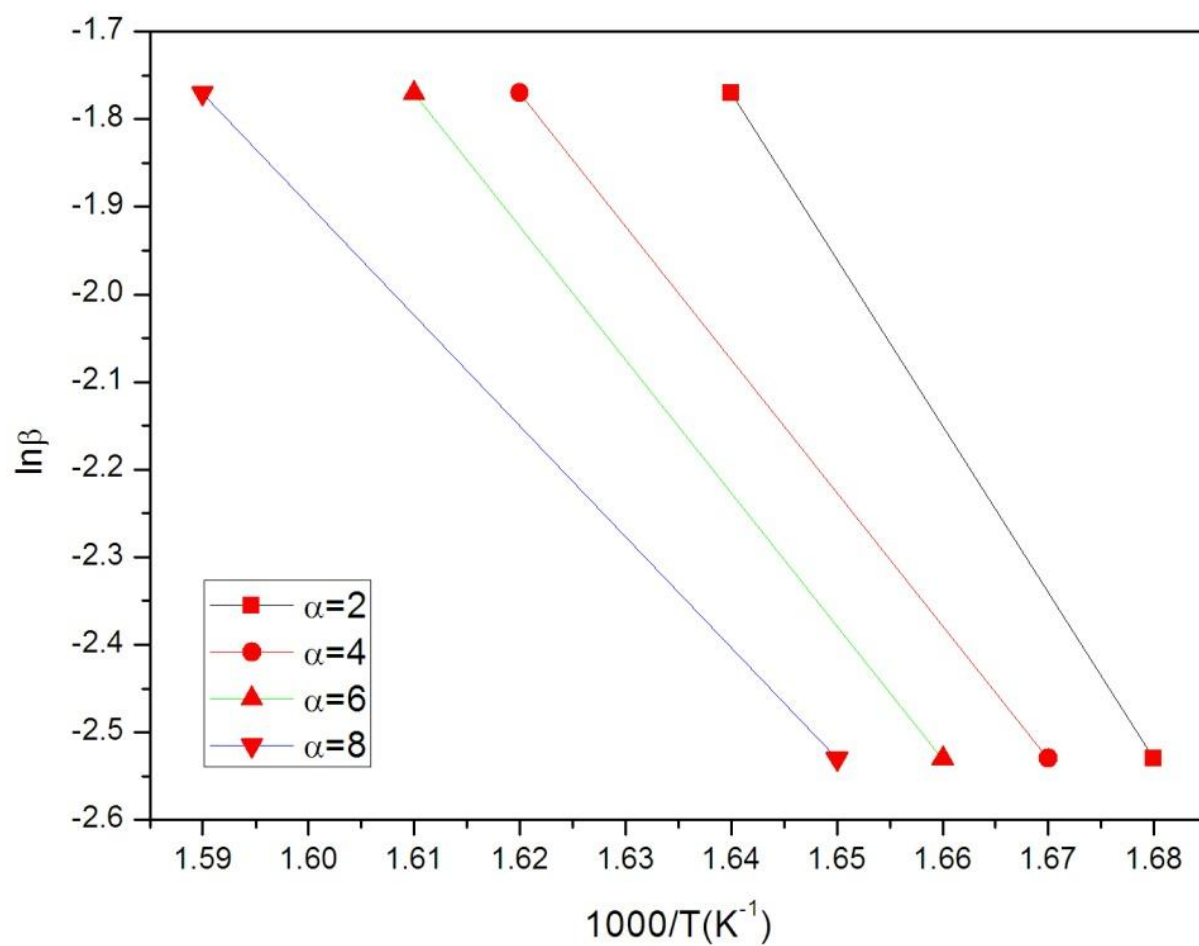


Fig. 5.3: *OFW plots for ZBLAN glass*

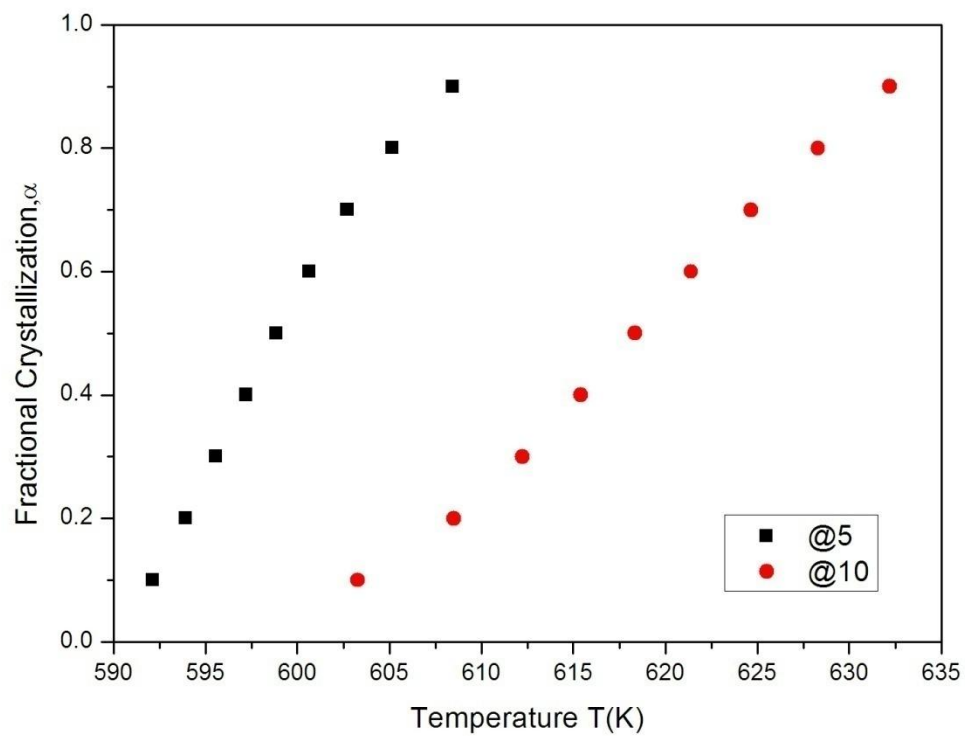


Fig. 5.4: *Fractional crystallization as a function of temperature at various heating rates for ZBLAN glass*

Crystallization Kinetics of $\text{Co}_{65}\text{Si}_{15}\text{B}_{14}\text{Fe}_4\text{Ni}_2$ (2714A) Metallic Glass

[The cobalt based metallic glass $\text{Co}_{65}\text{Si}_{15}\text{B}_{14}\text{Fe}_4\text{Ni}_2$ has good soft magnetic properties. Metallic glass 2714A with composition $\text{Co}_{65}\text{Si}_{15}\text{B}_{14}\text{Fe}_4\text{Ni}_2$, is used in high frequency electromagnetic devices, shows very good soft magnetic properties [10].]Ref-1)[such as low coercivity and low hysteresis loss and high permeability and high saturation magnetization. So, they are widely used in antitheft security system, magnetic recording heads, magnetic sensors, large transformers and electronic devices [4.48- 4.52]. The nano-crystalline state has also been obtained from Co-based amorphous precursors [4.53, 4.54]. From recent reports, it is clear that Co based metallic glass is suitable for its use in magnetic sensors [4.55].]A)[Many researchers [11-14] have reported the annealing effects on magnetic properties of this alloy. In this study, we will report the crystallization behavior of $\text{Co}_{65}\text{Si}_{15}\text{B}_{14}\text{Fe}_4\text{Ni}_2$ in more detail. Ref-1)

The DSC thermograms at four different heating rates are shown in Fig. 5.1. The thermograms show single step crystallization. The crystallization peaks for heating rates 5, 10, 15 and 20 $^{\circ}\text{C}/\text{min}$ are found to be at 822.31, 830.08, 834.16 and 835.69 K respectively.

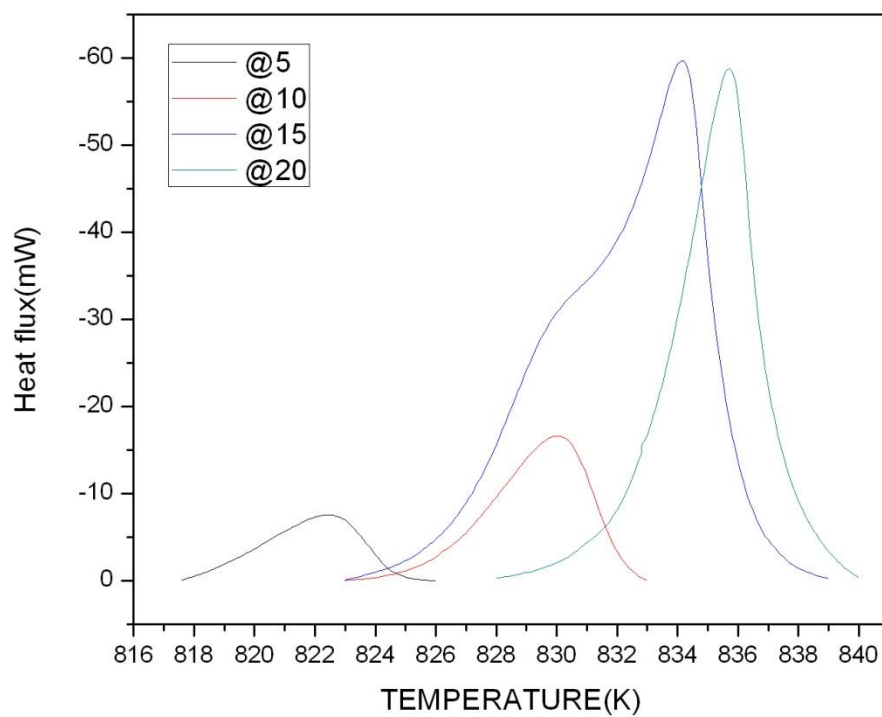


Fig.5.1 DSC thermograms of the metallic glass $\text{Co}_{66}\text{Si}_{12}\text{B}_{16}\text{Fe}_4\text{Mo}_2$ at different two heating rates

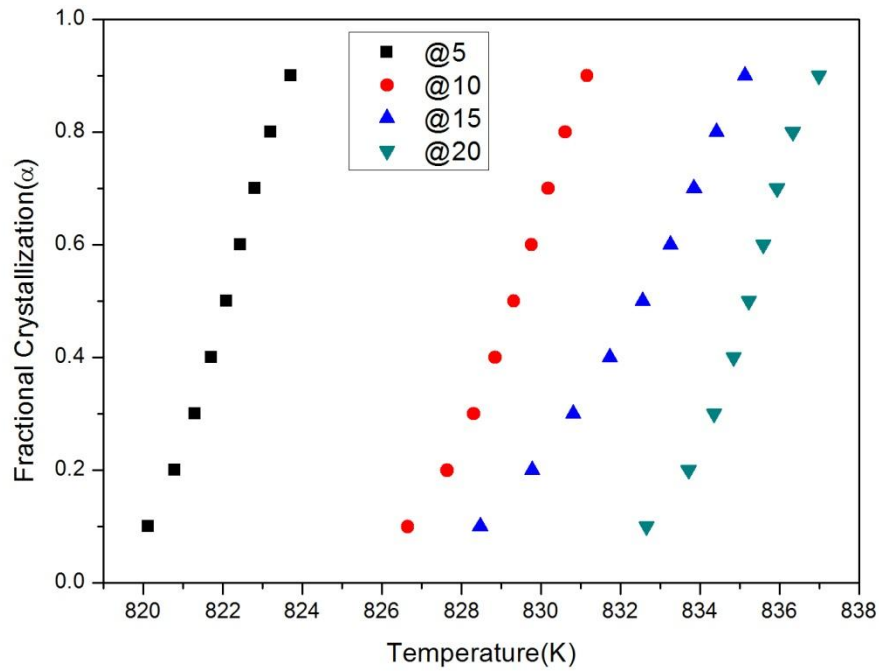


Fig. 5.2: Fractional crystallization as a function of temperature at various heating rates for $\text{Co}_{65}\text{Si}_{15}\text{B}_{14}\text{Fe}_4\text{Ni}_2$ metallic glass

Figure 5.2 shows the graphical representation of the volume fraction transformed (α) as a function of temperature (T) for different heating rates. The sigmoid plot exhibits the bulk crystallization and excludes the chance of surface crystallization. During the stage “a” nucleation occurs at various points in the bulk of the sample. In the stage “b” the growth of nuclei with increased rate of reaction as the surface area of nucleation increases. The slowing down stage “c” shows the decrease in surface area as a result of nuclei coalescing. [H]

Linear Integral Isoconversional Methods

Using the linear integral isoconversional methods given by OFW and KAS the activation energy at different extent of conversion (fractional crystallization) have been evaluated (Table 5.3). Figures 5.3 & 5.4 show the plots for OFW [Eq. (5.5)] and KAS [Eq. (5.6)] methods for $\alpha = 0.2, 0.4, 0.6$ and 0.8 . The E values obtained from both the methods decreases initially then increases and afterwards again decreases. The shift in the crystallization peak with increasing heating rate is used to obtain the activation energy from Kissinger and Ozawa methods. Figs 5.17 and 5.18 show the Kissinger and Ozawa plots. The Kissinger method assumes that the reaction rate is maximum at

the peak temperature (T_p) (Table 5.1). This assumption implies a constant degree of conversion (α_p) at T_p . This method is grouped as a special case of KAS isoconversional method. Referring to Eq. (5.7) a plot of $\ln(\beta/T_p^2)$ Vs. $1000/T_p$ (Fig. 5.5) gives an approximate straight line with the slope (E/R) and the intercept $\ln(AR/E)$. A single value of E is obtained at $T = T_p$ from the Ozawa plot [Eq. (4.5)] of $\ln\beta$ Vs. $1000/T_p$ as in Fig. 4.6. The so obtained activation energy from both Kissinger and Ozawa methods are 553 kJ/mol and 546 kJ/mol respectively (Table 5.2). Table 5.1 Peak temperature, T_p and onset temperature, T_o for four different heating rates for $\text{Co}_{65}\text{Si}_{15}\text{B}_{14}\text{Fe}_4\text{Ni}_2$

Heating rates β (K/min)	T_o (K)	T_p (K)
5	818.31	822.31
10	826.27	830.08
15	830.41	834.16
20	833.14	835.69

Using Eq. (5.10) for Boswell method, from the slope of the graph $\ln(\beta/T_p)$ Vs. $1000/T_p$ (Fig. 5.7) the value of E is determined as 443 kJ/mol. The Augis and Bennett method [Eq. (5.8)] uses the peak crystallization temperature and onset crystallization temperature (Table 5.1) to evaluate E and A . The plot of $\ln(\beta/T_p - T_o)$ Vs. $1000/T_p$ (Fig. 5.8) gives the values of E as 532 kJ/mol.

Table 5.2 Activation energy (E) derived using various methods for $\text{Co}_{65}\text{Si}_{15}\text{B}_{14}\text{Fe}_4\text{Ni}_2$

Methods	E (kJ/mol)
Kissinger	550.46 \pm 4.95
Ozawa	537.67 \pm 5
Augis& Bennett	693.63 \pm 17.11
Bosewell	558.45 \pm 5.2

Table 5.3 Local Activation energy (E) at different conversion for different methods

α	$E_a(\text{kJ mol}^{-1})$		
	KAS	OFW	
0.1	624.96 \pm 10.17	607.35 \pm 10.18	
0.2	624.96 \pm 7.28	607.74 \pm 7.16	
0.3	619.38 \pm 3.9	602.38 \pm 3.81	
0.4	618.89 \pm 3.9	602.38 \pm 3.81	
0.5	609.9 \pm 3.23	593.76 \pm 3.04	
0.6	609.46 \pm 0.7	592.81 \pm 0.78	
0.7	595.91 \pm 5.5	580.09 \pm 5.4	
0.8	597.77 \pm 2.8	582.07 \pm 2.79	
0.9	597.26 \pm 2.5	550.235 \pm 2.34	

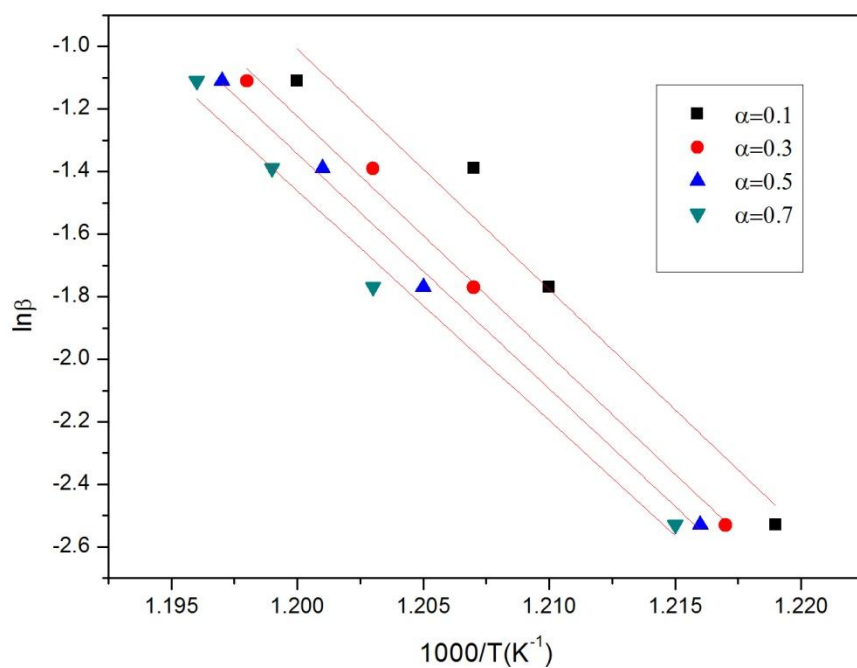


Fig. 5.3: OFW plots for $\text{Co}_{65}\text{Si}_{15}\text{B}_{14}\text{Fe}_4\text{Ni}_2$

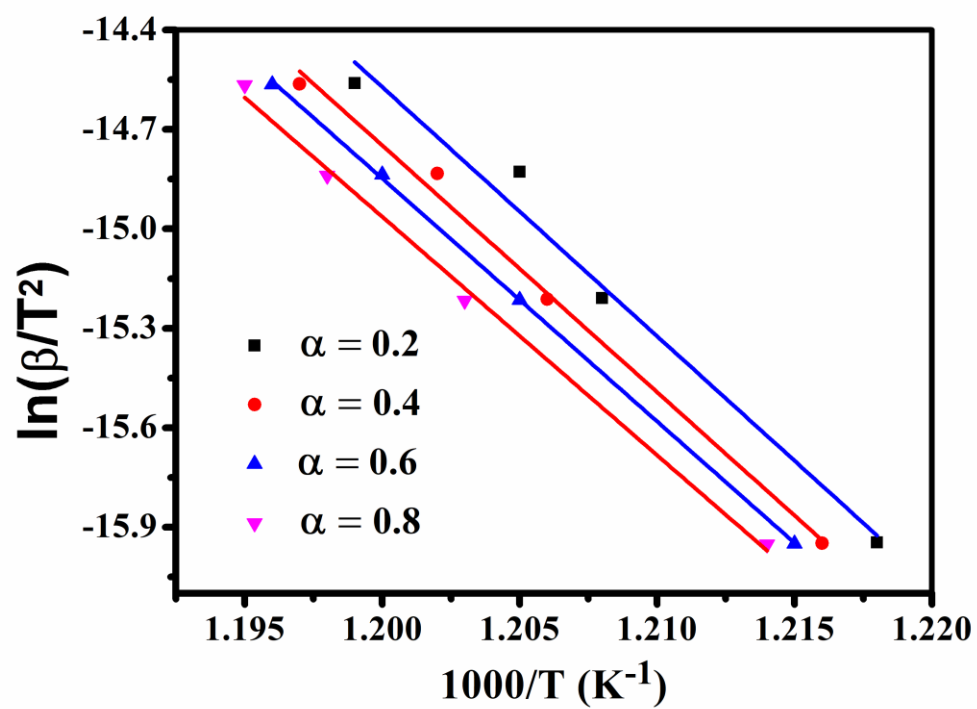


Fig. 5.4: KAS plots for $Co_{65}Si_{15}B_{14}Fe_4Ni_2$

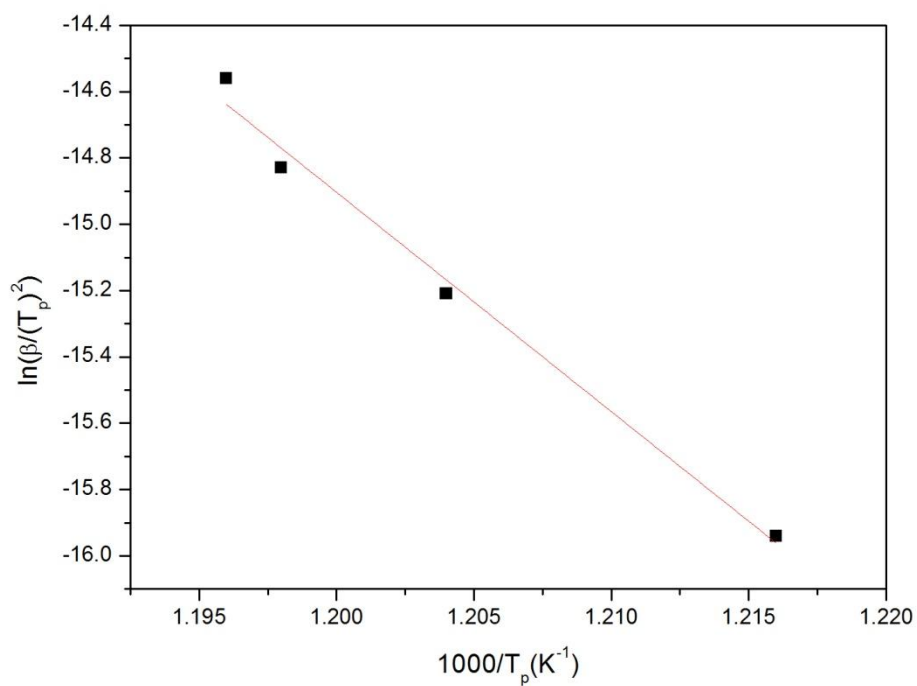


Fig. 5.5: Kissinger plot for Co₆₅Si₁₅B₁₄Fe₄Ni₂

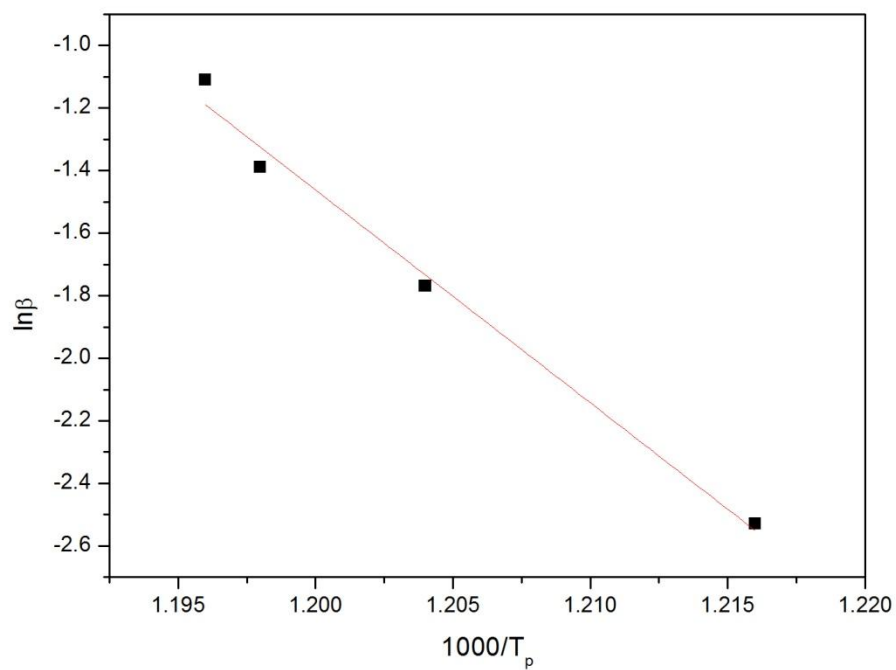


Fig. 5.6 Ozawa plot for Co₆₅Si₁₅B₁₄Fe₄Ni₂

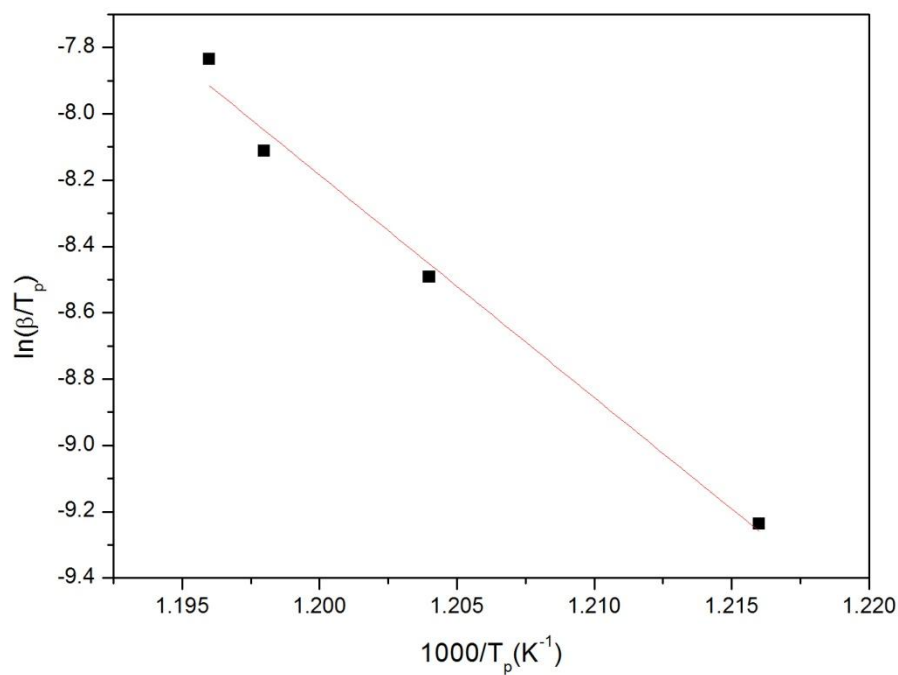


Fig. 5.7 Boswell plot for $Co_{65}Si_{15}B_{14}Fe_4Ni_2$

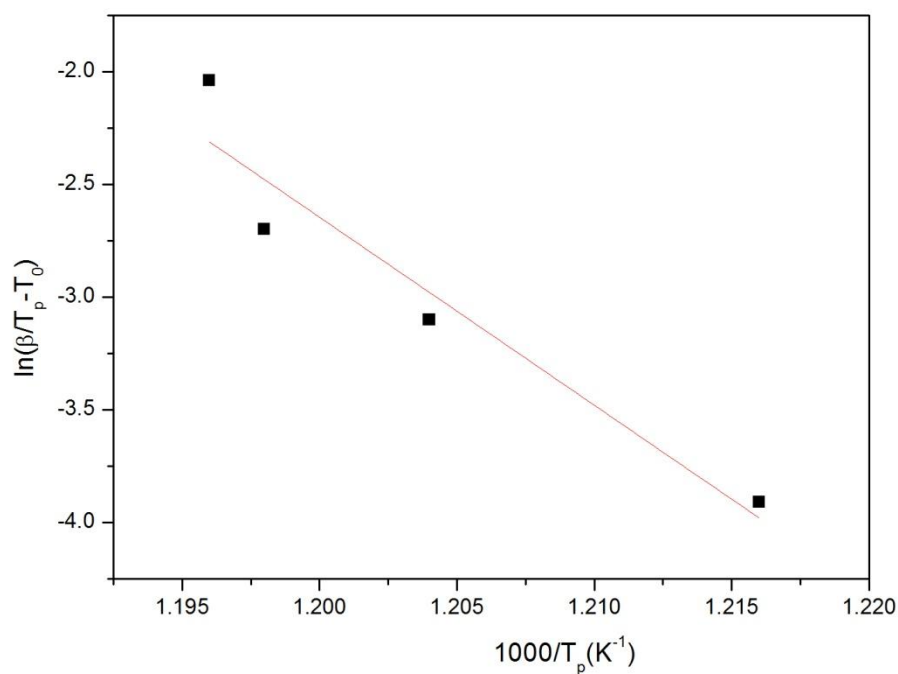


Fig. 5.8 Augis & Bennett plot for $Co_{65}Si_{15}B_{14}Fe_4Ni_2$

Crystallization Kinetics of ZBLAN Glass

In the present work, the kinetics of the crystallization of the ZBLAN glass has been studied.

Fluorozirconate glasses are potential candidates for opticaltelecommunication devices because of their low phonon energy andwide optical transmission window, ranging from the UV to the midinfrared. They are desirable materials forup-conversion lasers, optical amplifiers, and display devices [1–5].The fluorozirconate system, notably the ZrF₄-BaF₂-LaF₃-AlF₃-NaF(ZBLAN) glass composition, is one of the most stable against

devitrification among the fluoride glasses [6].]ref.2)

The DSC thermograms at four different heating rates (5, 10 deg/min) are shown in Fig. 5.13. The thermograms show two and three-stage crystallization process. Thepeak height of these steps varies with the heating rate. At lower heating rates, both peaks are much distinct and diminishes as we go for higher heating rates. In the present paper, the first peak is taken

into consideration for the kinetic analysis. Glass transition temperature is very evident in both thermograms. The analysis of DSC data to evaluate the kineticparameters can be obtained from non-isothermal rate laws by isoconversional (model independent) methods.

The plots of α Vs. T for different heating rates are shown in Fig. 5.14. The graphical representation of the volume fraction transformed (α) as a function of temperature (T) show the typical sigmoidal curves, which exhibit the bulk crystallization and exclude the chance of surface crystallization.

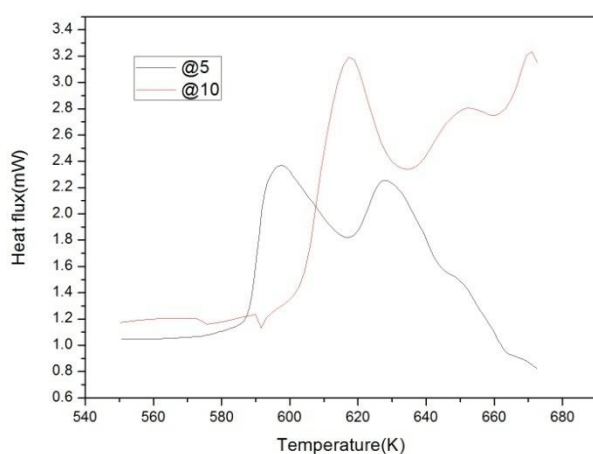


Fig.5.9 DSC thermograms of the ZBLAN glass at different heating rates

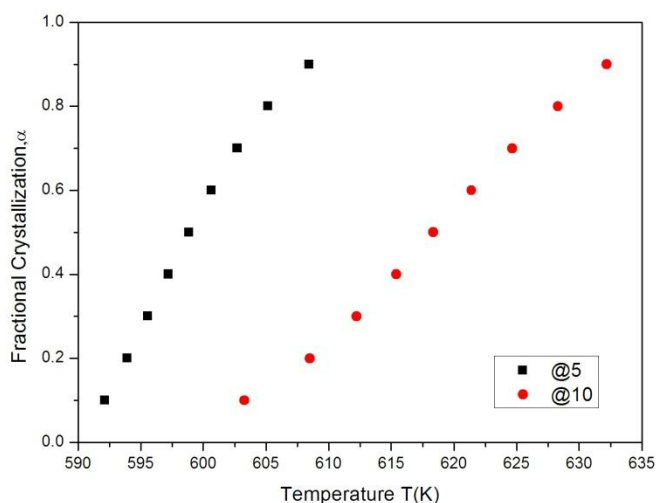


Fig. 5.10: Fractional crystallization as a function of temperature at various heating rates for ZBLAN glass

Linear Integral Isoconversional Methods

The values of local activation energy at particular α value are calculated using the OFW [Eq.(4.5)] and KAS [Eq.(4.6)] methods. The plots are shown in Figs. 5.15 and 5.16 and the values of E are listed in Table 4.7. It is observed that the activation energy continuously increases as α changes from 0.1 to 0.9, in case of both the methods.

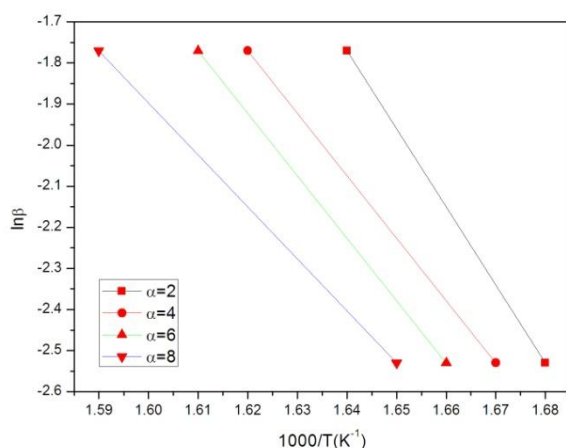


Fig. 5.11: OFW plots for ZBLAN glass

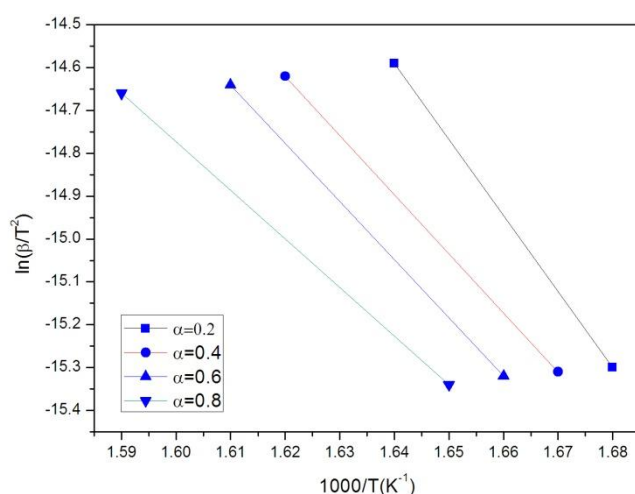


Fig. 5.12: KAS plots for ZBLAN glass

Table 5.4 Local Activation energy (E) at different conversion for different methods

α	$E_a(\text{kJ mol}^{-1})$		
	KAS	OFW	
0.1	196.71	200.02	
0.2	196.71	105.21	
0.3	114.73	120.17	
0.4	114.73	120.17	
0.5	114.73	120.17	
0.6	113.07	120.17	
0.7	94.20	100.09	
0.8	94.20	100.09	
0.9	94.20	100.09	

5.6 Conclusions

The crystallization behavior of Co65Si15B14Fe4Ni2 metallic glass and ZBLAN glass is studied under non-isothermal heating conditions using DSC. The kinetic parameters are evaluated using the isoconversional methods for both glasses.

The values of activation energy determined at different conversion, α using the linear integral isoconversional methods (OFW, KAS and Li & Tang) are found to be consistent. Integral isoconversional methods use integrals which describe the history of the system in the range α equal to 0.1 to 0.9.

Also it can be seen from Figures 5.12 and 5.31, that the values of local activation energy, E calculated using linear integral isoconversional methods show a decreasing trend as α changes from 0.1 to 0.9. This may be due to the fact that the crystallization

is a single step process in case of both the systems. So initially at small α values the nucleation rate is high and the activation energy here is due to both nucleation and growth. Hence high value of E is observed at lower α values. While towards the end of the process growth rate is more and the activation energy is mainly due to growth resulting in lower values of E . Model free isoconversional methods have been utilized to study the crystallization kinetics of the crystallization process involved in the presently taken systems namely $\text{Co}_{65}\text{Si}_{15}\text{B}_{14}\text{Fe}_4\text{Ni}_2$ and ZBLAN glasses. Isoconversional techniques provide quite accurate values of $E\alpha$ as a function of α as these analytical methods are supposed to be model free. It is also noteworthy that the activation energy values using various isoconversional methods and the special cases of isoconversional techniques namely Kissinger, Ozawa, Augis & Benett, Boswell and Gao & Wang are quite consistent, whereas modified Kissinger method overestimates it. For Co-based metallic glass, the activation energy obtained through KAS and OFW methods, decreases. The special cases of isoconversional methods namely Kissinger, Ozawa, Augis & Bennett & Boswell give quite consistent results and modified Kissinger methods also incorporate with them. Isoconversional methods provide activation energy values, E as a function of conversion, α . For metallic glasses, the thermally activated phase transformations are more physical than chemical. In fact, crystallization is a complex process involving nucleation and growth and on rigorous grounds, it cannot be considered to be a single-step process. The isokinetic analysis always leads to a single activation energy (rather say, apparent activation energy) giving an overall picture of the crystallization process. However, the difficulty (and hence uncertainty) in choosing the proper reaction model persists in isokinetic analysis. Therefore, the isoconversional methods are definitely superior to the isokinetic methods as far as the determination of E is concerned [5.56].

References

References

- [5.1] M. Castro, *Physical Review B* **67**; 2003: pp. 035412.
- [5.2] R.A. Ligeró, J. Vazquez, P. Villares, and R. Jimenez-Garay, *Thermochim. Acta*, **162**; 1990: pp. 427.
- [5.3] A.H. Moharram, M.A. El-Oyoun, and A.A. Abu-Sehly, *J. of Phys. D App. Phys.* **34**; 2001: pp. 2541.
- [5.4] N. Rysava, T. Spasov and L. Tichy, *J. Therm. Anal.* **32**; 1987: pp. 1015.

- [5.5] A. Giridhar, and S. Mahadevan, *J. Non-Cryst. Solids* **51**; 1982: pp. 305.
- [5.6] S. Afify, *J. Non-Cryst. Solids* **128**; 1991: pp. 279.
- [5.7] K.N. Lad, R.T. Savalia, Arun Pratap, G.K. Dey and S. Banerjee, *Thermochim. Acta* **473**; 2008: pp. 74.
- [5.8] A.T. Patel and Arun Pratap, *J. Therm. Anal. and Calorim.* **107**; 2012: pp. 159.
- [5.9] A.K. Galwey, *Thermochim. Acta* **399**; 2003: pp. 1.
- [5.10] S. Vyazovkin, *Thermochim. Acta* **397**; 2003: pp. 269.
- [5.11] M. E. Brown, D. Dollimore and A. K. Galwey, *Reactions in the Solid State. Comprehensive Chemical Kinetics*, Vol. 22. Amsterdam: Elsevier. 1980, 340 pp.
- [5.12] T. B. Brill and K. J. James, *Chem. Rev.* **93**; 1993: 2667–92
- [5.13] J. H. Flynn, In *Encyclopedia of Polymer Science and Engineering*, ed. HF Mark, NM Bikales, CG Overberger, G Menges, 1989, pp. 690–723 (Suppl.). New York: Wiley
- [5.14] D. W. Van Krevelen, *Coal. Typology Physics - Chemistry - Constitution*. Amsterdam: Elsevier, 1993
- [5.15] J. Sestak, *Thermophysical Properties of Solids. Comprehensive Analytical Chemistry*, Vol. 12D. Amsterdam: Elsevier. 1984: pp 440.
- [5.16] J. G. Fatou, In *Encyclopedia of Polymer Science and Engineering*, ed. HF Mark, NM Bikales, CG Overberger, G Menges, 1989, pp. 231–96 (Suppl.). New York: Wiley
- [5.17] J. H. Peperzko, In *Thermal Analysis in Metallurgy*, ed. RD Schull, A Joshi, 1992, pp.121–53. Warrendale, PA: TMS
- [5.18] D. Dollimore, *Anal. Chem.* **68**; 1996: R63–R71
- [5.19] S. Arrhenius, *Z. phys. Chem.*, **4**; 1889: 226.
- [5.20] C. N. Hinshelwood, *The Kinetics of Chemical Change in Gaseous Systems* (London: Oxford University Press). 1926
- [5.21] S. Vyazovkin and C. A. Wight, *Annu. Rev. Phys. Chem.* **48**; 1997: 125.
- [5.22] S. Vyazovkin and D. Dollimore, *J. Chem. Inf. Comput. Sci.* **36** (1); 1996: 42.

- [5.23] T. Ozawa, *Bull. Chem. Soc. Jpn.***38**; 1965: 1881.
- [5.24] J. H. Flynn and L. A. Wall, *J. Res. Natl. Bur. Stand. A. Phys. Chem.***70A**; 1966: 487.
- [5.25] H. E. Kissinger, *Anal. Chem.* **29**; 1966: 1702.
- [5.26] T. Akahira and T. Sunose, *Research report (Chiba Institute of Technology) Sci Technol.***16**; 1971: 22.
- [5.27] A. Augis and J. E. Bennett, *J. Therm. Anal. Calorim.* **13**; 1978: 283.
- [5.38] P. G. Boswell, *J. Therm. Anal. Calorim.* **18**; 1980: 353.
- [5.29] H. L. Friedman, *J. Polym. Sci.* **C6**; 1964: 183.
- [5.30] Y. Q. Gao and W. Wang, *J. Non. Cryst. Solids.* **81**; 1986: 129.
- [5.31] T. Ozawa, *Polymer*, **12** (1971) 150.

- [5.32] J. Bonastre, L. Escoda, J. Saurina, J.J. Sunol, J.D. Santos, M.L. Sanchez and B. Hernando, *J. Non-Cryst. Solids* **354**; 2008: pp. 5126.
- [5.33] J.S. Blazquez, M. Millan and C.F. Conde, *Phil. Mag.* **87**; 2007: pp. 4151.
- [5.34] J.J. Sunol, N. Clavaguera, M.T. Clavaguera-Mora, *J. Therm. Anal. Calorim.* **52**; 1998: pp. 853.
- [5.35] F. Paulik , *Special Trends in Thermal Analysis ; John Wiley & Sons , Chichester ,UK (1995) Ch. 10*
- [5.36] J. H. Flynn, L. A. Wall, *J. Res. Natl. Bur. Standards, A Phys. Chem.,* **70A** (1966) 487.
- [5.37] T. Ozawa, *Bull. Chem. Soc. Jpn.* **38** (1970) 1881.
- [5.38] T. Akahira, T. Sunose, *Res. Report, Chiba. Inst. Technol (Sci. Technol.)* **16** (1971) 22.
- [5.39] P. Murray, J. White, *Trans. Brot. Ceram. Soc.* **54** (1955) 204.
- [5.40] J. A. Augis, and J. E. Bennett, *J. Thermal Analysis*, **13** (1978) 283.
- [5.41] C. R. Li, T. B. Tang, *Thermochimica Acta*, **325** (1999) 43.
- [5.42] H. L. Friedman, *J. Polym. Sci.,* **C6** (1964) 183.
- [5.43] Y. Q. Gao and W. Wang , *J. Non-Crystalline Solids*, **87** (1986) 129.
- [5.44] S. Vyazovkin, *J. Comput. Chem.,* **18** (1997) 393.
- [5.45] Matusita, K. and Sakka, S., *Phys. Chem. Glasses*, **20** (1979) 81.
- [5.46] Matusita, K. and Sakka, S., *J. Non-Cryst. Solids*, **38-39** (1980) 741.
- [5.47] Coats, A.W. and Redfern, *Nature*, **201** (1964) 68.

- [5.48] Galwey, A. K., *Thermochim. Acta*, **399** (2003) 1.
- [5.49] Budrugeac, P., *J. Therm. Anal. Cal.*, **89**(2007) 143.
- [5.50] S.H. Lim, Y.S. Choi, T.H. Noh, I.K. Kang, *J. Appl. Phys.* 75 (1994) 6937.
- [5.51] I.C. Rho, C.S.Yoon, C.K.Kim, T.Y.Byun, and K.S. Hong, *J. Non-Cryst. Solids* **316**; 2003: pp. 289.
- [5.52] G. Buttino, A. Cecchetti and M. Poppi, *J. Magn. Magn. Mater.* **241**; 2002: pp. 183.
- [5.53] I.C. Rho, C.S. Yoon, C.K Kim, T.Y. Byun and K.S. Hong, *Mater. Sci. Engg. B* **96**; 2002: pp. 48.
- [5.54] Z.Z. Yuan, X.D. Chen, B.X. Wang and Z.J. Chen, *J. Alloy. Comp.* **399**; 2005: pp. 166.
- [5.55] G.Herzer, *IEEE Trans. Magn. Mag.* **26**; 1990: pp. 1397.
- [5.56] D.W Henderson *J.Non-Cryst. Solids* **30**; (1979):301.